Journal of Sound and Vibration (1998) **210**(5), 567–579

ESTIMATION OF OPERATIONAL STRAINS FROM VIBRATION MEASUREMENTS: AN APPLICATION TO LEAD WIRES OF CHIPS ON PRINTED CIRCUIT BOARD

S.-W. Seo, K.-J. Kim and B.-K. Bae

Center for Noise and Vibration Control, Department of Mechanical Engineering, KAIST, Korea

(*Received* 3 *September* 1996, *and in final form* 15 *September* 1997)

Dynamic strain in structures is normally measured using strain gauges. When direct strain measurement is not possible, vibration measurement can be an indirect practical alternative. That is, vibrations are measured, typically using acceleration pick-ups, on the underlying system under operational conditions and a certain relationship between strains and accelerations is imposed on the measured accelerations to estimate the strains. Therefore, this relationship or transformation matrix between the strain and vibration is very critical for the indirect estimation to be successful.

The transformation matrix is often inevitably derived not under the real operational conditions, but under the idealized laboratory conditions or using computer simulations. This means that boundary conditions under which this transformation matrix is obtained are extremely important. In this study, this problem is discussed in detail and an application to the estimation of strains in lead wires connecting chips to a printed circuit board subject to loading by a cooling fan is illustrated.

1. INTRODUCTION

When a structure is subject to dynamic forces, dynamic strain or stress develops in the structure and may lead the system to fatigue failure. The fatigue life of a structure is often determined by the highest strain or stress value in the structure, meaning that the strain or stress distribution must be known somehow under operational conditions in order to predict the fatigue life. Typically, strains are measured by attaching strain gauges onto the structure subject to the operational loading. Sometimes, however, the points of interest may not be accessible or it may be inappropriate to attach strain gauges. In such a case, it is necessary to employ an indirect method. Since the deflections of a structure and the strains in the structure are somehow interrelated, research work has been carried out to extract the strain information from the measured vibrations [1].

The relation between the vibration and the strain can be described by the so-called displacement-strain transformation matrix, which is ideally obtained from the experimental displacement and strain modal analysis on the structure under operational boundary conditions [1–3]. When experimental analysis under real operational conditions is not possible, it can be replaced with analysis under laboratory conditions or computational analysis. One problem with the alternative approaches is how to regenerate the real operational boundary conditions in the laboratory environment or how to describe

0022–460X/98/100567 + 13 $25.00/0/sv971327

them in mathematical terms in the computational approach. In this study, discussions will be made on the latter approach and its applications to the lead wires on a printed circuit board (PCB) will be presented where attachment of the strain gauge is not realizable.

2. BASIC BACKGROUND

When a continuous structure is subject to dynamic loading, its motion can be approximated by an n-degree-of-freedom system in matrix form as follows:

$$[M]\{\ddot{u}\} + [C]\{\dot{u}\} + [K]\{u\} = \{p\}, \tag{1}$$

where $[M]$, $[C]$ and $[K]$ are $n \times n$ mass, damping and stiffness matrices, respectively and $\{u\}$ and $\{p\}$ are $n \times 1$ displacement and force column vectors, respectively. Assuming only a small amount of damping, the operational displacements can be represented in terms of the normal modes of the undamped system as follows:

$$\{u\} = q_1\{\phi_1\} + q_2\{\phi_2\} + \cdots + q_n\{\phi_n\} = [\Phi]\{q\}, \tag{2}$$

where $[F]$, which has $\{f_i\}$ in the ith column, is called a displacement modal matrix.

Although strains in a structure are theoretically defined by derivatives of displacements with respect to spatial variables, it is assumed that the strains can be obtained approximately by multiplying a transformation matrix on the displacements. That is, operational strains in the structure are represented in matrix form as follows:

$$\{\varepsilon\} = [T]\{u\}, \tag{3}$$

where $\{\varepsilon\}$ and $[T]$ denote $e \times 1$ operational strain column vector and $e \times n$ displacement-to-strain transformation matrix, respectively. Furthermore, the transformation matrix $[T]$ is assumed to be constant regardless of the deformation shapes. Substitution of equation (2) into equation (3) gives

$$\{\varepsilon\} = [T][\Phi]\{q\} = [\Psi]\{q\}, \tag{4}$$

where $e \times n$ matrix $[\Psi]$ defined by

$$[\Psi] = [T][\Phi], \tag{5}$$

is the strain modal matrix [1–3]. Equation (5) implies that the displacement-to-strain transformation matrix $[T]$ is applicable to all of the dynamic modes equally and, hence, implies that the displacement-to-strain transformation matrix $[T]$ can be obtained in terms of the displacement and strain modal matrices:

$$[T] = [\Psi][\Phi]^{-1}. \tag{6}$$

The transformation matrix can be obtained from the displacement and strain modal analysis either by experiments in the laboratory environment or by the computational approach. The computational approach may be a must rather than a choice when attachment of strain gauges on the points of interest of the underlying structure is not physically possible. A typical computational method could be modelling and analysis of the system using the finite element method (FEM). One important problem here is, as mentioned in the introduction, how well one models the actual operational conditions in the FEM approach, because the transformation matrix derived under boundary conditions different from those of the real operations does not guarantee the success of this approximation technique. Thus, it is necessary to work on the choice of boundary conditions.

3. PREDICTION OF STRAINS UNDER ARBITRARY BOUNDARY CONDITIONS

3.1. DISPLACEMENT MODAL MATRIX UNDER OPERATIONAL BOUNDARY CONDITIONS

In the basic background above, the displacement-to-strain transformation matrix was discussed for a lumped parameter system and, hence, not much mention was made on the boundary conditions. Real structures are all continuous systems and the vibration problems must be described in terms of equations of motion as well as boundary conditions, which means that boundary conditions must be involved somehow in deriving the displacement-to-strain transformation matrix. The problem here is that, under actual operational conditions, the exact boundary conditions are seldom known. In such a case, approximate solutions are obtained by assuming the solution to be a superposition of basis functions which satisfy the equation of motion and any relevant boundary conditions available. That is, the response $\{u\}$ under actual operational loading and unknown boundary conditions is assumed to be the superposition of basis vectors, $\{f_i\}_c$'s, as follows:

$$\{u\} \cong [\{\phi_1\}_c, \ldots, \{\phi_i\}_c, \ldots, \{\phi_n\}_c]\{\alpha\} = [\Phi_c]\{\alpha\}, \tag{7}$$

where the basis functions are normal modes which satisfy equations of motion of the continuous system and properly assumed boundary conditions and $\{\alpha\}$ is a coefficient vector.

In order to illustrate the validity of this approach, consider transverse vibrations of a uniform beam with three different boundary conditions as shown in Figure 1: model A: free–free boundary condition at $x = 0, 1$; model B: clamped–free boundary condition at $x = 0, 1$; model C: spring supported–free boundary condition at $x = 0, 1$. A few lower mode shape vectors in each case are now going to be approximated using those under free or clamped boundary conditions. In order to do so, two sets of lowest 20-mode shape vectors were obtained for models A and B by using a commercial FEM program; then each set is used to obtain the approximate mode shapes for the other models.

Figure 2 shows the results for the lowest two modes. Figure 2(a) and (b) show that mode shapes for the infinite (model B) and a finite (model C) stiffness at the left end can be fairly well described using those for the zero stiffness at the end (model A). Figure 2(c) and (d) show that mode shapes for the zero (model A) and a finite (model C) stiffness at the left end obtained using those for the infinite stiffness at the end (model B) are fairly good also, except for the regin close to the left end. This example shows that mode shape vectors for the free boundary conditions are more desirable than those for the fixed ones. The results are very natural in a heuristic sense considering that the clamped end can be reproduced by the superposition of many free ends while the opposite case cannot be realized.

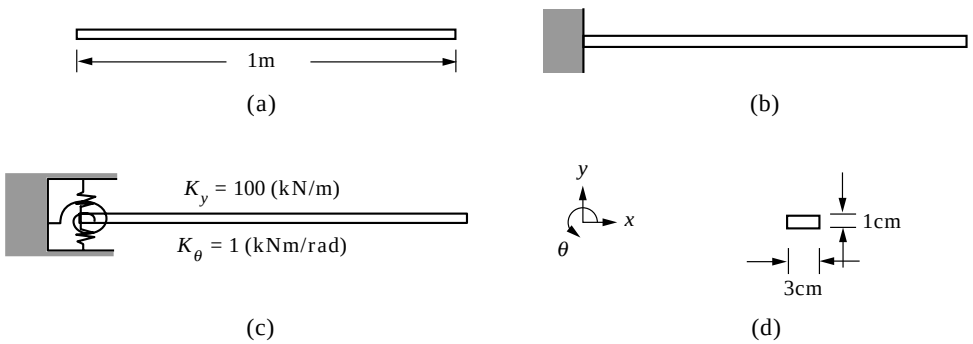

Figure 1. Three different boundary conditions at the left end of a beam: (a) model A; (b) model B; (c) model C.

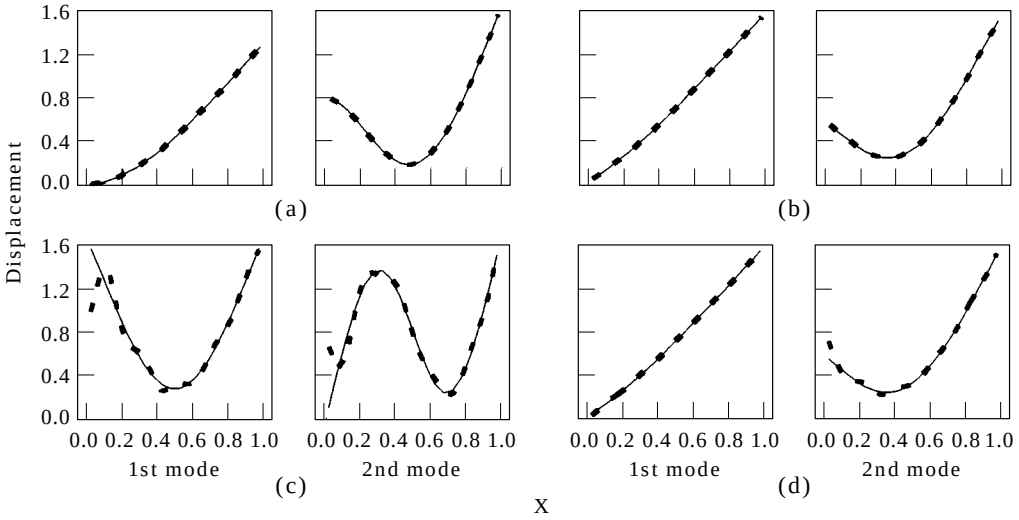

Figure 2. Approximation of modal vectors using basis vectors based on different boundary conditions: (a) for model B/from model A; (b) for model C/from model A; (c) for model A/from model B; (d) for model C/from model B. ——, Exact displacement modal vector; – – –, approximate displacement modal vector.

In this study, therefore, the deflection shape matrix is approximated under operational boundary conditions using the modal displacement matrix under free boundary conditions as follows:

$$[\Phi^{op}] \cong [\Phi^{fr}]\,[\beta], \tag{8}$$

where $[\Phi^{op}]$, $[\Phi^{fr}]$ and $[\beta]$ are the modal displacement matrix under operational boundary conditions, the modal displacement matrix under free boundary conditions and a coefficient matrix, respectively. Another problem to solve is to determine how many modes are desirable as basis vectors when the number of modes of interest is given under the operational boundary conditions. A simple way is to define an error as shown in Figure 3(a) and (b) and to observe the trend of the error reductions with the increase in the number of basis vectors. For example, a 5–10% error point can be chosen to determine the number of basis vectors.

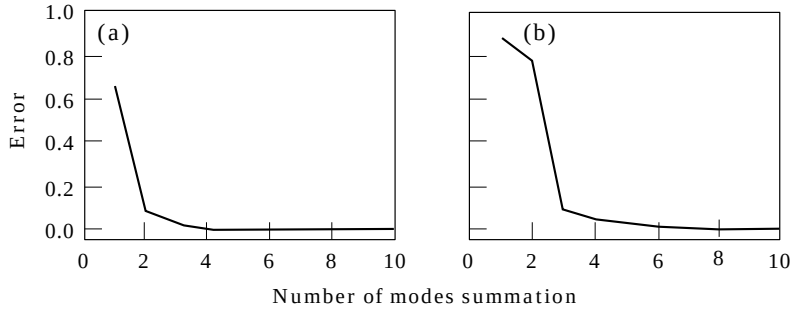

Figure 3. Error reductions with number of basis vectors: (a) 1st mode; (b) 2nd mode. Error = $\|\{\phi_i\} - \{\phi_i\}_c\|/\|\{\phi_i\}\|$, where $\{\phi_i\}$ is the ith displacement modal vector and $\{\phi_i\}_c$ is the ith approxmate displacement modal vector.

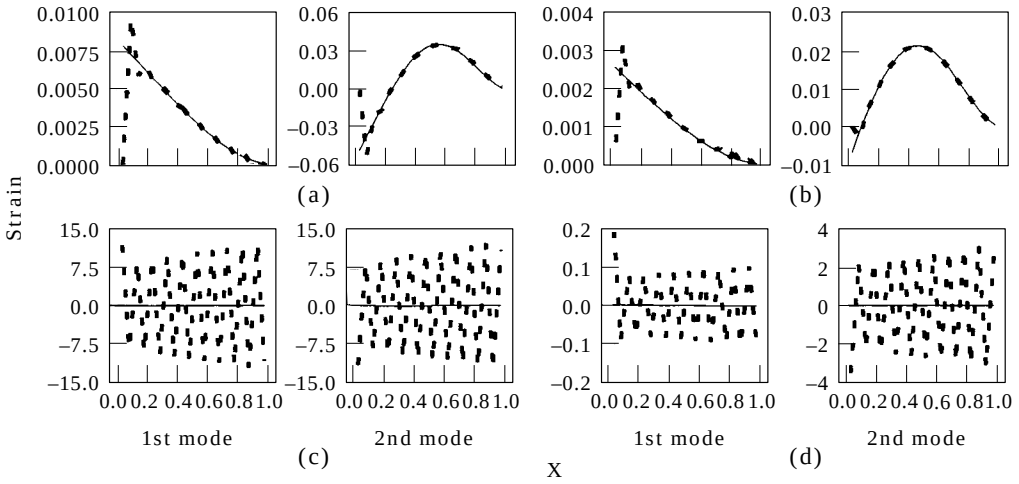

Figure 4. Prediction of strain modal vectors for a beam: (a) for model B/from model A; (b) for model C/from model A; (c) for model A/from model B; (d) for model C/from model B. ——, Exact strain modal vector; –––, approximate strain modal vector.

3.2. ESTIMATION OF OPERATIONAL STRAIN USING THE DISPLACEMENT-TO-STRAIN TRANSFORMATION

The operational displacements can be approximated by using the modal displacement vectors under free boundary conditions and the modal strains can be predicted by pre-multiplying the modal displacements with the modal displacement-to-strain transformation matrix. This means that the operational strain can be estimated from the operational displacements by using the transformation matrix under the free boundary conditions. That is, modal strains under free boundary conditions are related to the modal displacements under the same boundary conditions as follows:

$$[\Psi^{fr}] = [T^{fr}]\,[\Phi^{fr}]. \tag{9}$$

The transformation matrix obtained from equation (9) is used to approximate the modal as well as operational strain:

$$[\Psi^{op}] = [T^{fr}]\,[\Phi^{op}] = [\Psi^{fr}]^{-1}[\Phi^{fr}]\,[\Phi^{op}], \tag{10}$$

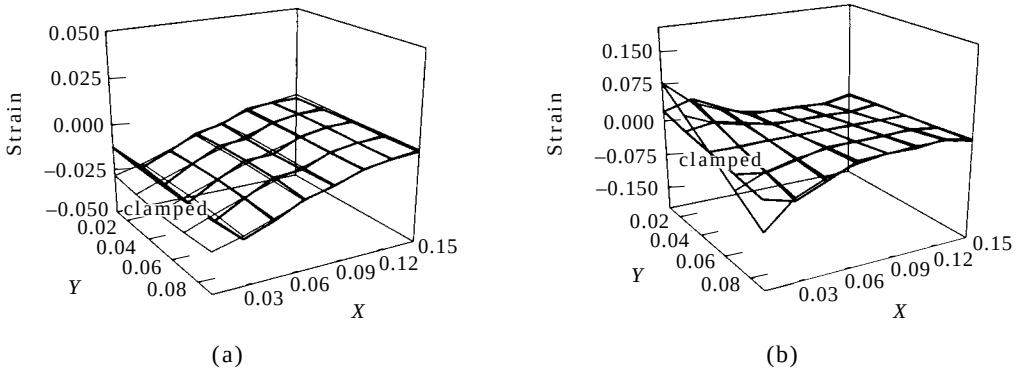

Figure 5. Prediction of strain modal vectors for a plate: (a) 1st mode; (b) 2nd mode. ——, Exact strain modal vector; ——, predicted strain modal vector.

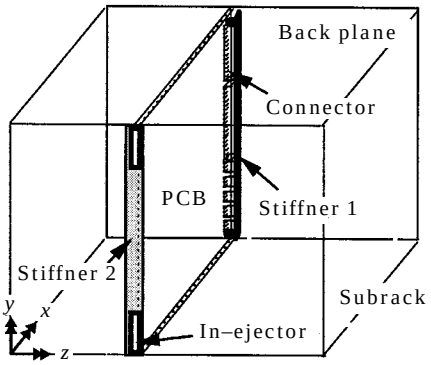

Figure 6. Configuration of subrack of an ATM system.

$$\{\varepsilon^{op}\} \cong [T^{fr}]\{u^{op}\} = [\Psi^{fr}]^{-1}[\Phi^{fr}]\{u^{op}\}. \tag{11}$$

In order to see the validity of equation (10), the beam with three different boundary conditions are revisited here. Strain modal matrices for models B and C were directly computed using FEM and compared with those predicted using the transformation matrix under the free boundary conditions (model A). Figure 4(a) and (b) show strain distributions in the 1st and the 2nd modes for models B and C, where the dotted lines are the estimations based on the displacement-to-strain transformation matrix under the free boundary conditions, i.e., for model A while the solid lines are results directly obtained from FEM analysis under correct boundary conditions. No significant differences can be seen except at the left-hand boundary point where the beam is constrained by the stiffness so that stress concentration is inevitable to some extent. This will be discussed further in the next section. Figure 4(c) and (d) show similar results for models A and C, where the dotted lines are estimations based upon the transformation matrix obtained under clamped boundary conditions, i.e., for model B. Discrepancies of the estimations are so large that true strain distributions look almost negligible, i.e., the solid lines are very close to zero. One reason is that the displacements under the non-fixed boundary conditions cannot be represented well by using normal modes under the fixed boundary conditions as mentioned in the previous section. Another reason is that the strain level near the clamped end is so overwhelming when the basis functions are taken from the normal modes under the fixed boundary conditions that the strains in other areas of the beam are likely to be overestimated. In Figure 5 estimations are shown of stress distribution for a plate with clamped–free–free–free boundary conditions obtained by using the transformation matrix

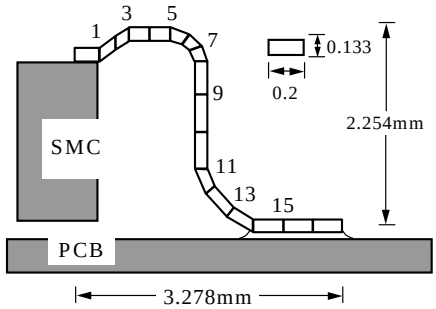

Figure 7. FEM model of a lead wire.

for a plate with free–free–free–free–boundary conditions. It can be seen that the thick solid lines (estimations) are fairly good when compared with the thin solid lines (exact values).

3.3. PROBLEMS IN BOUNDARY STRAIN PREDICTION

Although it is claimed in this study that one can get the displacement-to-strain transformation matrix better from the free boundary conditions than from the fixed conditions, this procedure has its own limitations in that the strains are not computed by the displacement derivatives with respect to spatial variables, but extracted from the displacements themselves in the linear least square sense. In this section, the problems in strain predictions near the boundary points are addressed.

Since strains are computed under free boundary conditions, elements of the top and bottom rows in the matrix $[\Psi^{fr}]$ in equation (9) are zeroes and, consequently, the top and bottom rows of the transformation matrix given by

$$\begin{bmatrix} T_{11} & T_{12} & \cdots & T_{1n} \\ \vdots & \vdots & T_{ij} & \vdots \\ T_{e1} & T_{e2} & \cdots & T_{en} \end{bmatrix} = \begin{bmatrix} 0 & 0 & \cdots & 0 \\ \vdots & \vdots & \Psi_{ij} & \vdots \\ 0 & 0 & \cdots & 0 \end{bmatrix} [\Phi]^{-1} \tag{12}$$

are zeroes. Thus, whatever the modal displacements under operational boundary conditions may be, modal strains become zeroes at the boundaries.

4. APPLICATION TO LEAD WIRES OF A SURFACE MOUNTED CHIP

Asynchronous transfer mode (ATM) telecommunications system, a leading edge equipment used for high speed electronic data transmission, has many components on the PCB. Cooling fans, which are driven by electric motors and attached on the frame in order

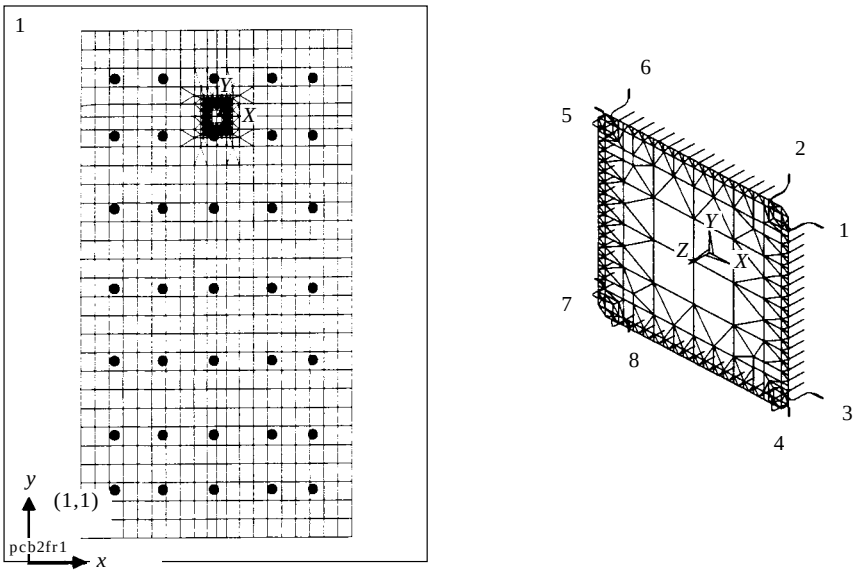

(a) (b)

Figure 8. FEM model of a PCB with SMC: (a) FE modelling of PCB; (b) FE modelling of SMC. (Ansys 5·0, 16 December 1995, 19:51:19, plot no. 1. ZV = 1, Dist = 0·2244, YF = 0·135, ZF = 0·004, centroid hidden.)

to remove the heat generated from the electronic components, bring about dynamic loading to the components. Lead wires of surface mount components (SMC) which connect the electronic components onto the PCB are one of the most probable points of failure by fatigue, so it is very important to know how high the strain levels are in the lead wires under operational conditions. However, it is impossible to measure the operational strains in lead wires directly by attachments of the strain gauges.

In this case study, the technique of displacement-to-strain transformation matrix is applied to the SMC by using a commercial FEM software. Figure 6 shows the configuration of a subrack of an ATM switching system in which PCBs are clamped by the connector at the back and by in-ejectors at the front. A rack consists of several subracks installed in the vertical direction. One set of cooling fans consisting of four fans is located at the top of the rack and another set at the bottom of the rack. In Figure 7, details of a spider gull wing lead wire soldered at the PCB and SMC are shown.

4.1. PREDICTION OF MODAL STRAINS IN LEAD WIRES UNDER ACTUAL BOUNDARY CONDITIONS

Figure 8(a) shows the FEM model of a PCB with a SMC on it and Figure 8(b) shows details of the SMC, where it can be seen that only eight lead wires at the corners are modelled by the "beam elements" as shown in Figure 7 and 100 lead wires at the edge are modelled by simple "spring elements" [4–6]. The reason for this simplification is that lead wires in the corner are known to be weaker than others [7, 8] and modelling of all lead wires by the "beam elements" would need a great deal of computation time and memory.

From the FEM analysis, modal displacements as well as modal strain distributions were obtained under the free–free–free–free boundary condition of the PCB, which can be related to each other in terms of the displacement-to-strain transformation matrix:

$$\begin{bmatrix} \Psi_{PCB} \\ \Psi_{lead} \end{bmatrix} = [T]\,[\Phi_{PCB}], \tag{13}$$

where $[\Psi_{PCB}]$ and $[\Phi_{PCB}]$ denote the strain and displacement modal matrices, respectively, for the PCB, and $[\Psi_{lead}]$ denotes the strain modal matrix for the lead wires. In this study,

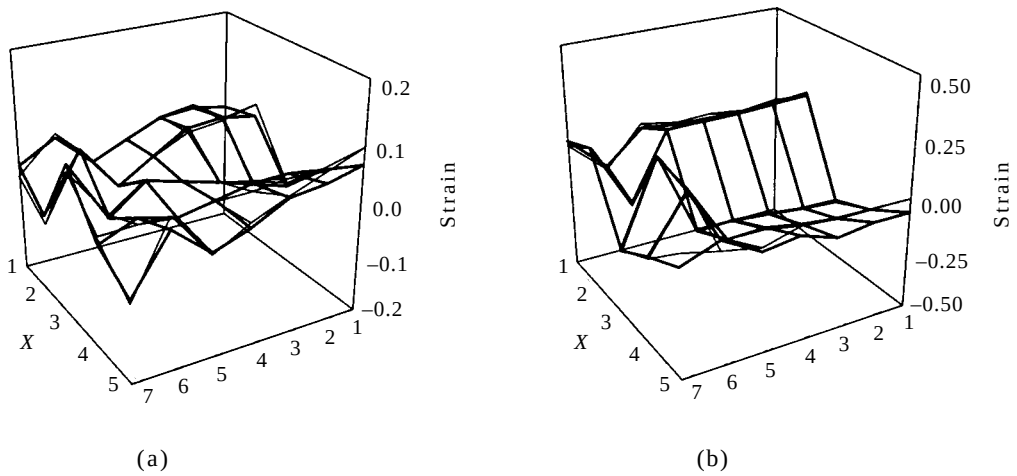

Figure 9. Predictions of modal strains for the PCB: (a) 1st mode; (b) 2nd mode. ——, Exact strain modal vector; ——, predicted strain modal vector.

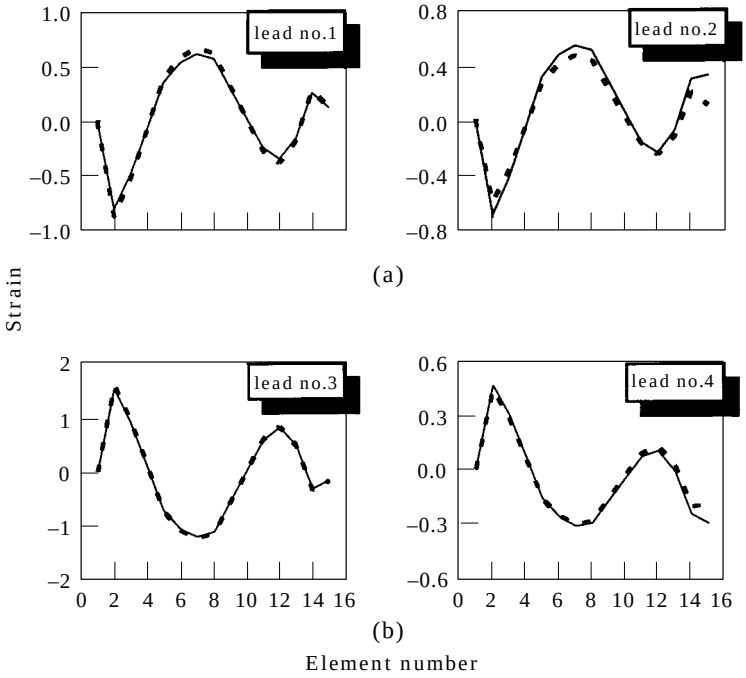

Figure 10. Predictions of modal strains for a lead wire: (a) 1st mode of PCB; (b) 2nd mode of PCB. ——, exact strain modal vector; –––, predicted strain modal vector.

the displacement modal matrix for the PCB was represented by 35 black-dotted points as shown in Figure 8(a) and that for the lead wires by 15 points on each of eight lead wires at the corners of the SMC, as shown in Figure 8(b). The number of modes to construct

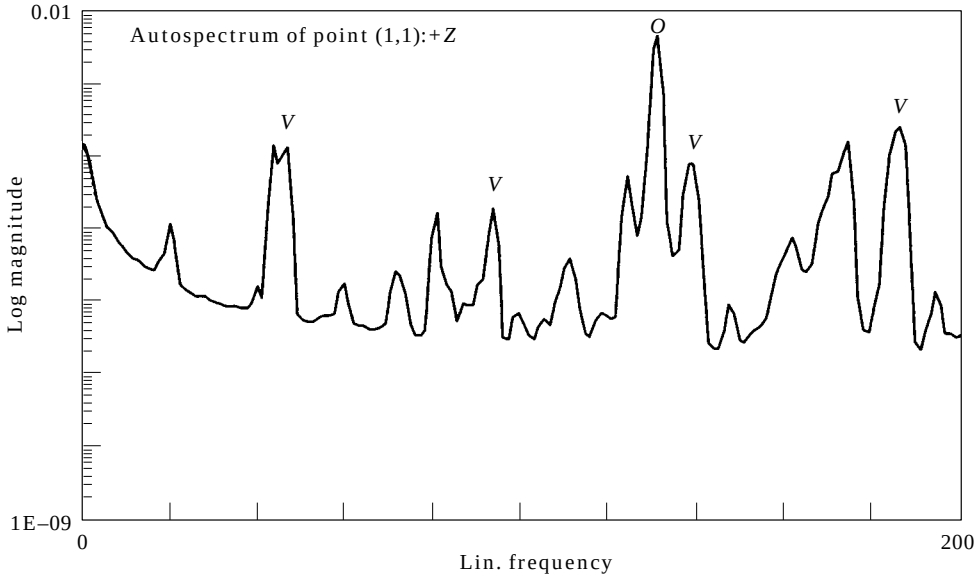

Figure 11. Power spectrum of acceleratins from point (1, 1).

the transformation matrix was 20. Thus, the 155 by 20 transformation matrix was obtained by using the pseudo-inverse of the 35 by 20 modal displacement matrix $[\Phi_{PCB}]$:

$$[T^{fr}] = \begin{bmatrix} \Psi^{fr}_{PCB} \\ \Psi^{fr}_{lead} \end{bmatrix} [\Phi^{fr}_{PCB}]^{+} \qquad \text{where } + : \text{pseudo-inverse.} \tag{14}$$

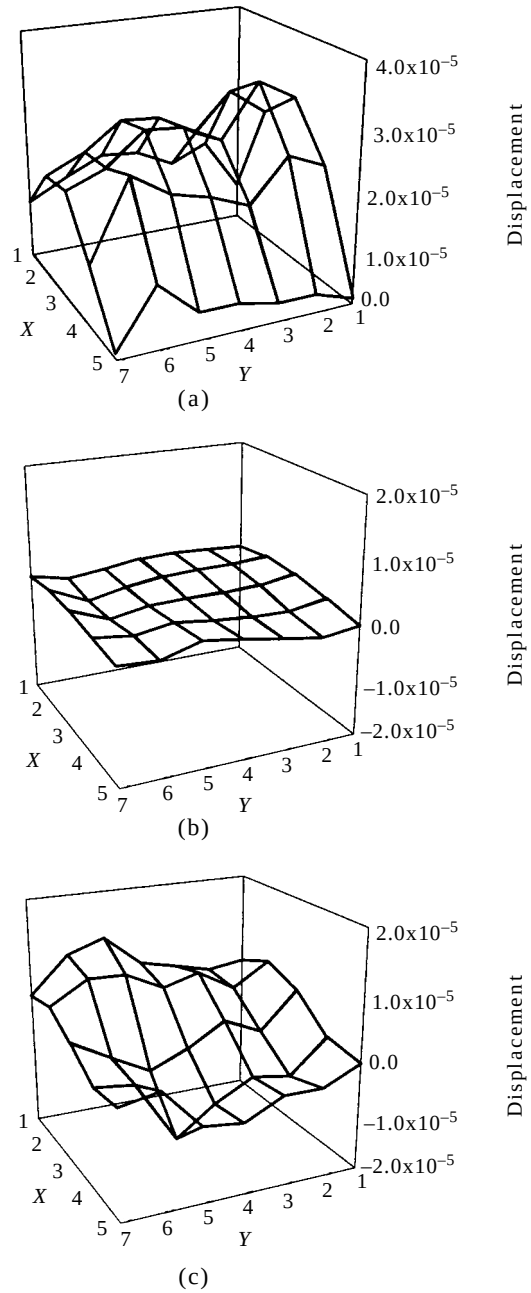

Figure 12. Operational deflection shapes of the PCB at three harmonic frequencies: (a) 46 Hz; (b) 92 Hz; (c) 131 Hz.

Before estimating the strains in lead wires under operational loading, the modal strains under actual operational boundary conditions of the PCB were predicted by using the transformation matrix and compared with the computation results directly obtained from the FEM analysis of the PCB under the operational boundary condition. Modelling of the boundaries for this analysis was based on very rigorous experimental analysis [9], where the boundaries were modelled by linear and rotational springs and the stiffness coefficients were tuned by comparing them with the measurements. Figure 9 shows the two results for the PCB; thick lines represent predicted strain mode shapes and thin lines, directly computed results. Figure 10 shows similar results for lead wires nos 1 and 2, where the element number on the abscissa means the number shown in Figure 7.

This result shows that the strains in lead wires subject to operational loading can also be predicted by pre-multiplying the operational displacement modes with the displacement-to-strain transformation matrix.

4.2. PREDICTION OF OPERATIONAL STRAINS IN THE LEAD WIRES

While four cooling fans rotate at about 2800 r.p.m. or 46 Hz to dissipate the heat generated from the chips, vibrations of the PCB were measured from 35 points on the board, as shown in Figure 8(a), by using accelerometers. Figure 11 shows the power spectrum of the accelerations at a point in the front bottom corner of the PCB, where the fundamental and higher harmonics of 46 Hz are marked by "*V*". Since rotational speeds of the four fans were not exactly the same, more than one peak can be observed for each

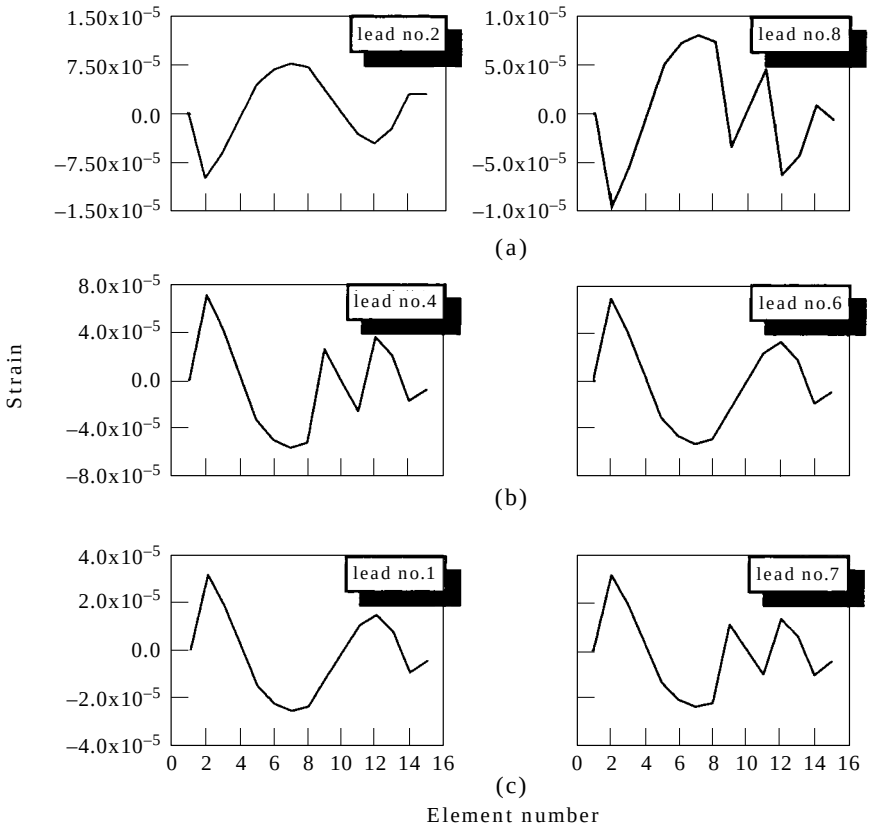

Figure 13. Predicted strain distribution in lead wires for each harmonic: (a) 46 Hz; (b) 92 Hz; (c) 131 Hz.

harmonic. The displacement spectrum by which one can get deformation severity information can be obtained by dividing the acceleration spectrum with the squares of frequency. Power of the displacement spectrum would then be concentrated in the low frequency range, which may mislead one to conclude that fatigue failure is more likely to occur at the fundamental frequency than at the higher harmonics. Since the strain is determined not by the displacment shape itself but by its spatial derivative, it should be carefully investigated which mode is most responsible for the failure. In Figure 12, deformation shapes at three harmonic frequencies are shown, where it is noted that deflections at the fundamental and the 3rd harmonic are almost of the same magnitude. Figure 13 shows the strain distributions in the two most heavily loaded leads at the three harmonics are larger than the other leads for each harmonic. It can be seen that, as a whole, element no. 2 or 3 of the leads is subject to the largest strain ($3{\cdot}0 \times 10^{-5}$) and the strain level at the 3rd harmonic is more significant than the others.

5. CONCLUSIONS

It has been shown that operational strains of a structure can be predicted from operational displacements and the displacement-to-strain transformation matrix, which can be obtained from experimental or numerical modal analysis for the strain and displacement under non-operational boundary conditions. It was shown that each displacement mode under arbitrary boundary conditions can be represented by summation of the modes under free boundary conditions more effectively than under other boundary conditions. Thus, in order to predict strains under operational conditions, it is recommended that the transformation matrix be obtained under free boundary conditions. As an application, the strains of lead wires of a SMC in the ATM system which is excited by the cooling fans are predicted to about $3{\cdot}0 \times 10^{-5}$, where the displacement-to-strain transformation matrix was obtained using FEM analysis.

REFERENCES

1. N. Okubo and K. Yamaguchi 1995 *Proceedings of the International Modal Analysis Conference* XIII, 91–96. Prediction of dynamic strain distribution under operating condition by use of modal analysis.
2. A. C. Pisoni and C. Santolini 1995 *Proceedings of the International Modal Analysis Conference* XIII, 119–125. Displacements in a vibrating body by strain gauge measurements.
3. O. Bernasconi and D. J. Ewins 1988 *Proceedings of the International Modal Analysis Conference* VI, 1453–1464. Application of strain modal testing to real structures.
4. R. W. Kotlowitz 1989 *IEEE Transactions on Components, Hybrids and Manufacturing Technology* **12**, 431–448. Comparative compliance of representative lead designs for surface-mounted component.
5. D. J. Ewins 1984 *Modal Testing*: *Theory and Practice*. New York: Research Studies Press Ltd, Wiley. See pp. 19–59.
6. L. Meirovitch 1967 *Analytical Methods in Vibration*. New York: Macmillan. See pp. 126–166.
7. P. A. Engel 1993 *Structural Analysis of Printed Circuit Board System*. Berlin: Springer-Verlag. See pp. 116–161.
8. Y. C. Fung 1965 *Foundations of Solid Mechanics*. Englewood Cliffs, NJ: Prentice-Hall. See pp. 334–339.
9. Electronics and Telecommunications Research Institute 1995 *Study on Design and Analysis of Vibration in ATM Telecommunication System*.

APPENDIX: LIST OF SYMBOLS

$[C]$ $(n \times n)$ damping matrix
$[K]$ $(n \times n)$ stiffness matrix
$[M]$ $(n \times n)$ mass matrix
$\{p\}$ $(n \times 1)$ force vector
$\{q\}$ $(n \times 1)$ modal coordinate vector
$[T]$ $(e \times n)$ displacement-to-strain transformation matrix
$\{u\}$ $(n \times 1)$ operational displacment vector
$\{a\}$ $(n \times 1)$ coefficient vector
$[b]$ $(n \times n)$ coefficient matrix
$\{\varepsilon\}$ $(e \times 1)$ operational strain vector
$[F]$ $(n \times n)$ displacement modal matrix
$\{f_i\}$ $(n \times 1)$ ith displacement normal mode vector
$[\Psi]$ $(n \times n)$ strain modal matrix
$\{y_i\}$ $(n \times 1)$ ith strain modal vector

Sub- and Superscripts

c approximate value for continuous system
op operational condition
fr free boundary condition
$Lead$ lead-wires
PCB printed circuit board
-1 inverse
$+$ pseudo-inverse